JOURNAL OF GEOPHYSICAL RESEARCH, VOL. 114, D09303, doi:10.1029/2008JD011524, 2009

Implications of the day versus night differences of water vapor, carbon monoxide, and thin cloud observations near the tropical tropopause

Chuntao Liu[1] and Edward J. Zipser[1]

Received 24 November 2008; revised 4 March 2009; accepted 9 March 2009; published 7 May 2009.

[1] There are some interesting day versus night differences in the water vapor and carbon monoxide concentrations near the tropopause over tropical land and ocean from 4 years of EOS Microwave Limb Sounder (MLS) observations. To interpret these differences, the diurnal cycle of deep convection reaching near tropical tropopause summarized from a decade of tropical rainfall measuring mission (TRMM) observations. We also present the diurnal cycle of the cold point tropopause temperature and height derived from 2 years of constellation observing system for meteorology ionosphere and climate (COSMIC) GPS temperature profiles, the day versus night differences of occurrence of thin clouds from 2 years of cloud-aerosol lidar and infrared pathfinder satellite observations (CALIPSO) and 16 years of stratospheric aerosol and gaseous experiment (SAGE) II. In the tropical upper troposphere, day versus night differences of water vapor and carbon monoxide are consistent with the diurnal cycle of the vertical transport of water vapor and carbon monoxide–rich air from the surface by deep convection. However, in the tropical tropopause layer (TTL) over land, day versus night differences of water vapor concentration are more consistent with the diurnal variations of temperature in a saturated TTL, which is related to the diurnal cycle of cooling in the TTL induced by deep convection. The day versus night differences of occurrences of thin clouds in the TTL are also consistent with the freeze drying, controlled by the diurnal cycles of temperature in the TTL.

Citation: Liu, C., and E. J. Zipser (2009), Implications of the day versus night differences of water vapor, carbon monoxide, and thin cloud observations near the tropical tropopause, *J. Geophys. Res.*, *114*, D09303, doi:10.1029/2008JD011524.

1. Introduction

[2] What controls the amount of water vapor transport from the troposphere to the stratosphere over the tropics? This has become a hot topic in the past decade. The main argument is the role of deep convection in the dehydration process in the upper troposphere and lower stratosphere, often referred to as the Tropical Tropopause Layer (TTL). While the concept of "freeze and dry" [*Brewer*, 1949] has been generally accepted, there are still arguments on whether the freezing is mainly due to large scale rising and cooling of the upper troposphere air into the stratosphere [*Hartmann et al.*, 2001; *Jensen and Pfister*, 2004], or due to adiabatic cooling by deep convection [*Newell and Gould-Stewart*, 1981; *Danielsen*, 1982; *Sherwood and Dessler*, 2003]. Another mystery is that through the freeze and dry process, the tropopause temperature controls the amount of water vapor passing through the tropopause. However, the observed decrease of tropical tropopause temperature in the past decades is difficult to reconcile with the increase of water vapor in the stratosphere over Boulder during the same time period [*Randel et al.*, 2000, 2006]. Because the cooling in the tropical lower stratosphere may be related to the strengthening of tropical convection, understanding the role of the deep convection on the temperature and the water vapor budget in the TTL becomes critical.

[3] Many attempts have been made to evaluate the impact of deep convection on the water vapor budget of the TTL, including model simulation [*Sherwood and Dessler*, 2003; *Fueglistaler and Haynes*, 2005; *Gettelman and Birner*, 2007; *Jensen et al.*, 2007], water isotope analysis [*Dessler et al.*, 2007], and geoseasonal correlations between water vapor and the deep convection [*Massie et al.*, 2002; *Gettelman et al.*, 2002; *Dessler et al.*, 2006; *Liu et al.*, 2007a]. In this study, we seek another important signature of deep convection in water vapor observations: the diurnal cycle.

[4] The diurnal cycle is one of the main characteristics of tropical deep convection, with the afternoon maximum over land, and the early morning maximum but a weaker cycle over ocean [*Hall and Vonder Haar*, 1999; *Dai*, 2001; *Yang and Slingo*, 2001; *Nesbitt and Zipser*, 2003]. Using 10 years of observations from TRMM, *Liu and Zipser* [2008] pointed out that the amplitudes of diurnal cycles of occurrence of precipitation increase with height and the diurnal cycle of occurrence of precipitation is the strongest in the upper troposphere. Therefore if deep convection plays an important role in the water vapor budget of the TTL, there should be some day-night differences in the water vapor observations

[1]Department of Meteorology, University of Utah, Salt Lake City, Utah, USA.

0148-0227/09/2008JD011524$09.00

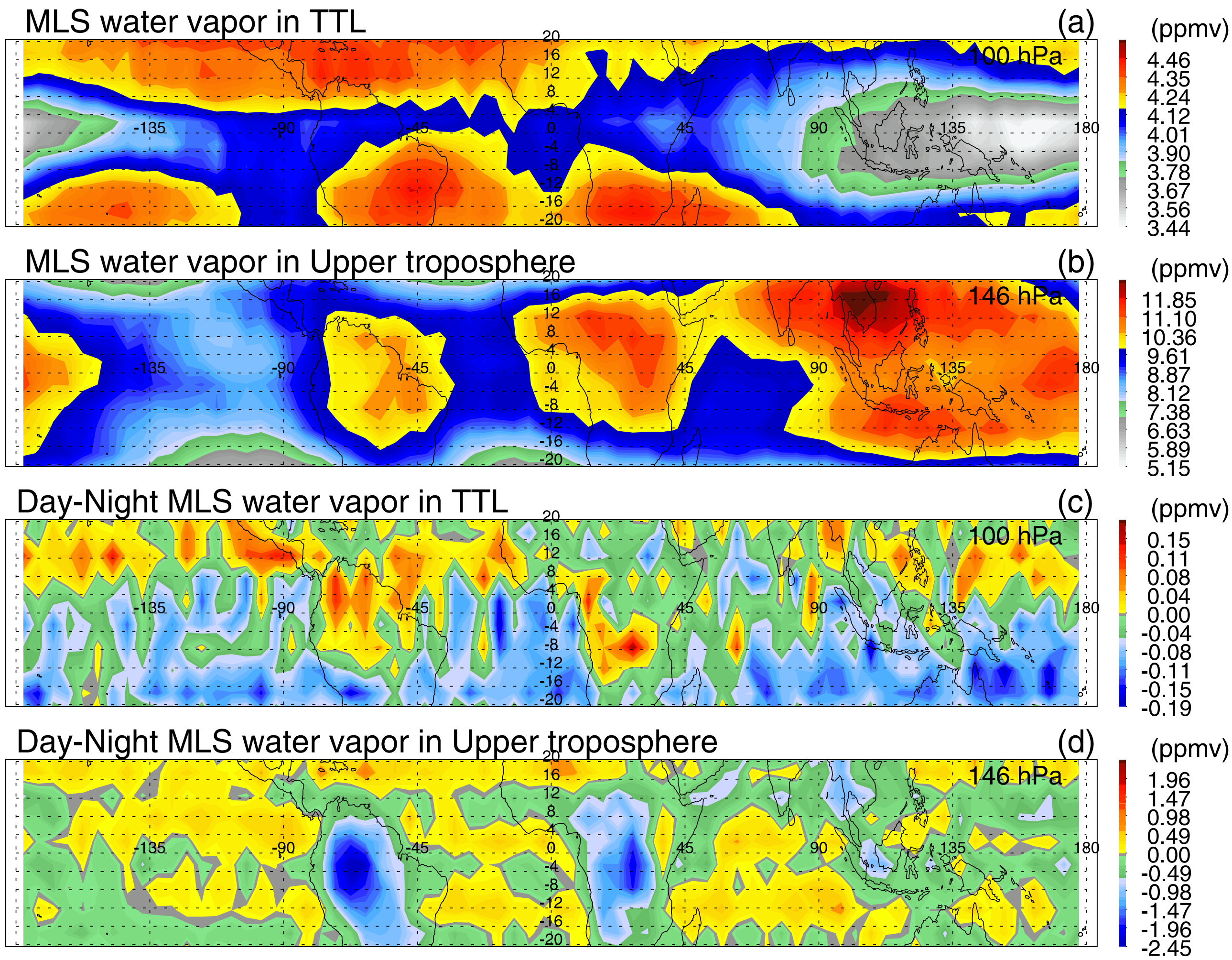

Figure 1. Mean water vapor mixing ratio and their day versus night differences at 146 and 100 hPa for 4 years (2005–2008) of AURA MLS observations. (a) Mean water vapor mixing ratio at 100 hPa. (b) Same as Figure 1a, but at 146 hPa. (c) Differences between mean water vapor mixing ratio at 0130 and 1330 at 100 hPa. (d) Same as Figure 1c, but at 146 hPa.

in the upper troposphere and the TTL, especially over tropical land.

[5] Figure 1 shows the geographical distribution of mean water vapor mixing ratios and their differences between day (1330 local time) and night (0130 local time) at 100 hPa and 146 hPa from four years of AURA Microwave Limb Sounder (MLS) observations. The mean height of 100 hPa, and 146 hPa between 10°S–10°N are 16.6 km in the TTL, and 14.4 km near the bottom of the TTL with 1 standard deviation about 0.03 km according to 2.5° resolution NCEP reanalysis data.). Indeed, there are large day versus night differences (Figure 1d) with up to 20% higher water vapor concentration at 0130 than at 1330 over Amazon and central Africa at 146 hPa. However, there is lower water vapor concentration at 0130 than at 1330 (Figure 1c) over the same land regions at 100 hPa.

[6] Carbon monoxide (CO) has a photochemical life time of weeks to months in the troposphere and is often used as a tracer for vertical and horizontal transport near the tropopause [e.g., *Kar et al.*, 2004]. Since CO is insoluble and immune from the dehydration process, it can be used to facilitate understanding of the driving mechanisms behind water vapor concentrations near the tropopause [*Duncan et al.*, 2003; *Ricaud et al.*, 2007; *Liu et al.*, 2007a]. For example, the seasonal cycles of water vapor and CO in the stratosphere are negatively correlated [*Schoeberl et al.*, 2006]. Mean CO mixing ratio and the differences from 1330 to 0130 at 100 hPa and 146 hPa are shown in Figure 2. Similar to the day versus night differences of water vapor concentration at 146 hPa (Figure 1d), there is more CO at 0130 than at 1330 at 146 hPa over tropical land (Figure 2d). However, there is more CO at 0130 than at 1330 over central Amazon and Africa (Figure 2c), the opposite of water vapor day versus night differences at 100 hPa (Figure 1c). These observations lead to the main questions we address in this study:

[7] 1. Can we use diurnal cycles of deep convection to interpret the day-night differences in the amount of water vapor and carbon monoxide at 146 hPa and 100 hPa?

[8] 2. To be specific, why are there higher concentrations of water vapor and CO at 0130 than at 1330 over tropical land at 146 hPa in general (Figures 1d and 2d)?

[9] 3. Why is there higher concentration of water vapor at 1330 than at 0130 over tropical land (e.g., Africa) at

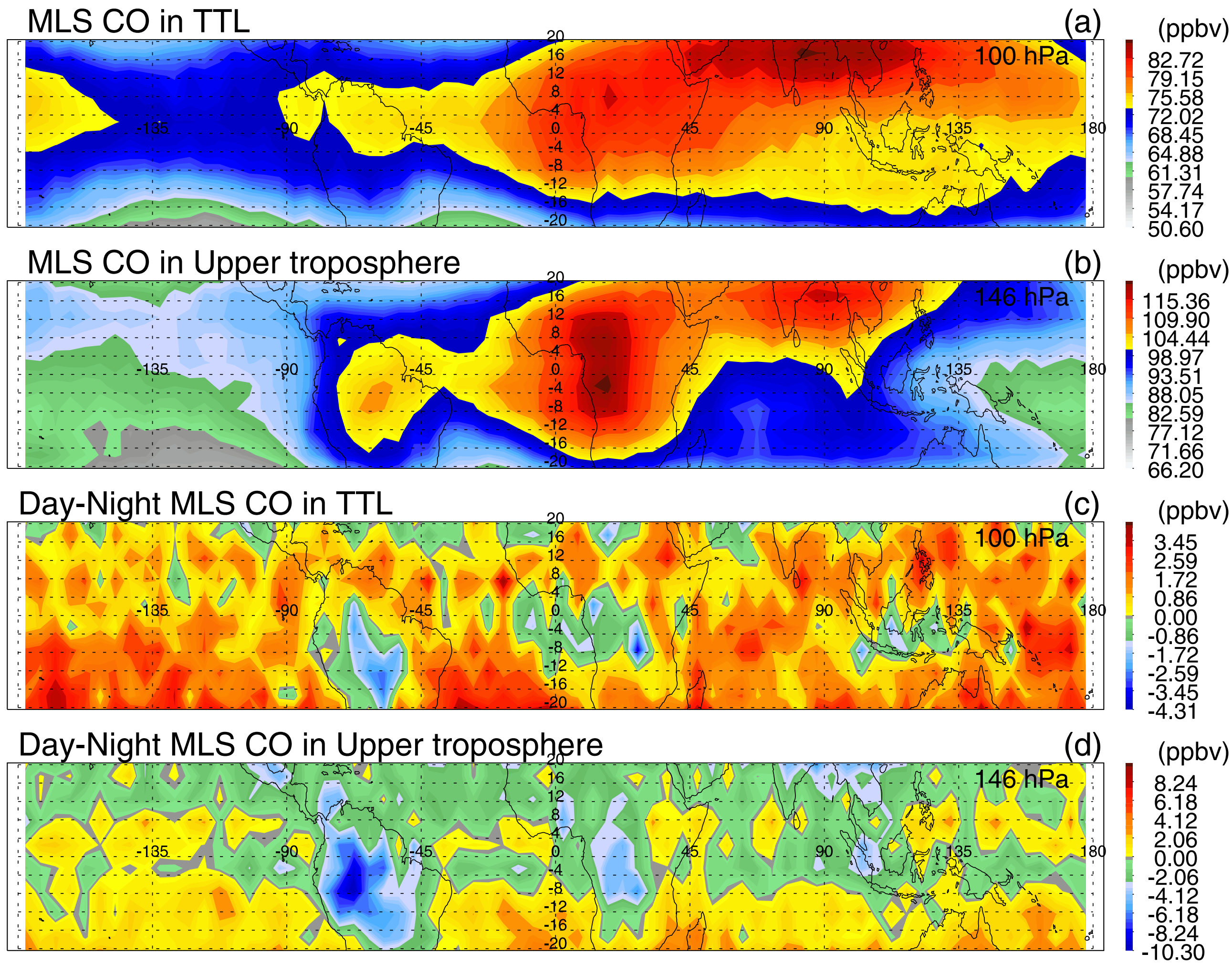

Figure 2. Mean carbon monoxide (CO) mixing ratio and their day versus night differences at 146 and 100 hPa for 4 years (2005–2008) of AURA MLS observations. (a) Mean carbon monoxide mixing ratio at 100 hPa. (b) same as Figure 2a, but at 146 hPa. (c) Differences between mean carbon monoxide mixing ratio at 0130 and 1330 at 100 hPa. (d) Same as Figure 2c, but at 146 hPa.

100 hPa (Figure 1c), which is opposite to that of CO (Figure 2c)?

[10] Since ice clouds are directly generated during the freeze-dry process in the TTL, it is important to relate the day versus night differences of cloud amount in the TTL to the diurnal variations of water vapor. In general, the clouds in the TTL may be from three sources: (1) Clouds with large precipitation size particles in the core of deep convection. There is evidence that these clouds are rare (~0.01% from 20°S–20°N) but sometimes can reach above the Cold Point Tropopause (CPT [*Liu and Zipser*, 2005; *Corti et al.*, 2008]). (2) Anvil clouds generated from outflow of deep convection. These clouds often occur near the bottom of the TTL and are detectable by satellite infrared images. (3) Thin subvisual clouds with low optical depth. These clouds occur frequently (20–50%) over the tropics [*Wang et al.*, 1996] and may have a large impact on the radiation balance [*Sassen et al.*, 1989]. They are possibly generated through the large scale circulation or gravity waves [*Hartmann et al.*, 2001; *Potter and Holton*, 1995]. Independent of cloud processes, the tropopause temperature itself is one main factor controlling the amount of water vapor in the TTL.

[11] In this study, the geodiurnal variations of deep convection and their thick anvil reaching the TTL from are generated from 10 years Tropical Rainfall Measuring Mission (TRMM [*Kummerow et al.*, 1998]). The day versus night differences of thin clouds are presented from two years of Cloud-Aerosol Lidar and Infrared Pathfinder Satellite Observations (CALIPSO [*Winker et al.*, 2003]) and 16 years of Stratospheric Aerosol and Gaseous Experiment (SAGE [*McCormick et al.*, 1995]) II. The geodiurnal variations of CPT temperature and height are summarized from two years of Constellation Observing System for Meteorology Ionosphere and Climate (COSMIC [*Anthes et al.*, 2008]) GPS radio occultation observations. Then the impact of the diurnal cycle of deep convection on the TTL are evaluated based on these observations to explain the day versus night differences in the concentrations of water vapor and CO in Figures 1 and 2.

2. Data

[12] Concentrations of water vapor and CO in the TTL are available from retrievals of EOS MLS measurements

[*Livesey et al.*, 2006, 2007] onboard the AURA satellite. The MLS can provide water vapor and CO measurements in the TTL with vertical resolution of 2–4 km and global coverage. The precisions of water vapor and CO concentration retrievals in the TTL (100 hPa) are about 15% and 30% respectively. Since the data set opened to the public, EOS MLS water vapor and CO observations have been widely used in the TTL and the lower stratosphere studies [e.g., *Schoeberl et al.*, 2006; *Jiang et al.*, 2007; *Read et al.*, 2008]. Here monthly mean water vapor and CO mixing ratios at 146 hPa and 100 hPa in $10^\circ \times 10^\circ$ grids in Figures 1 and 2 are calculated from four full years (2005–2008) of version 2.2 MLS retrievals. All MLS data used in this paper are processed with criteria described by *Livesey et al.* [2007].

[13] To identify the tropical deep convection in the TTL, 10 years of TRMM Precipitation Radar (PR) and Visible and Infrared Scanner (VIRS) data are matched and grouped into Precipitation Features (PFs) and Cloud Features (CFs) by pixels with PR reflectivity greater than 20 dBZ and the VIRS 10.8 μm wavelength brightness temperature (T_{B11}) < 210 K separately. Then the characteristics of the PFs and CFs, such as area of 20 dBZ PR reflectivity at 14 km and area of T_{B11} < 210 K, are summarized. *Liu et al.* [2008] described this method and demonstrated that there are large regional differences of tropical deep convection viewed from infrared radiometer and radar [*Liu et al.*, 2007b]. In this study, the area of T_{B11} < 210 K in CFs is used to indicate the thick anvil area of deep convection reaching the TTL. The mean height of the 210 K level between 10°S–10°N is 13.6 km ± 0.14 km (one standard deviation) according to the 2.5° resolution NCEP reanalysis [*Kistler et al.*, 2001]. The area of PR 20 dBZ reaching 14 km inside CFs is used to indicate core of deep convection with penetration into the TTL [*Liu and Zipser*, 2005]. Since TRMM has a non sunsynchronous orbit, it provides a good diurnal sampling of the deep convection in the tropics [*Negri et al.*, 2002].

[14] The thin ice clouds in the TTL are radiatively important [e.g., *Sassen et al.*, 1989; *McFarquhar et al.*, 2000; *Hartmann et al.*, 2001]. Thus there have been many efforts to measure them using different techniques. These include limb view satellite instruments [e.g., *Wang et al.*, 1996; *Massie et al.*, 2002; *Wu et al.*, 2005], aircraft [*McFarquhar et al.*, 2000], and space-borne lidar [*Dessler et al.*, 2006]. In this study, to provide information on the diurnal variations of thin clouds, two independent measures of thin clouds sampled at four different local times are used. First is the thin cloud detected with limb viewing SAGE II observations during solar occultation events by using an algorithm similar to the cloud detecting algorithm developed by *Kent et al.* [1993]. The subvisual clouds in the TTL are identified from version 6.2 SAGE II data during 1985–2004, excluding the years (1991–1995) with contamination by volcanic aerosols [*McCormick et al.*, 1995]. The SAGE II satellite has a sunsynchronous orbit with overpasses near 0600 and 1800 local time. Cloud occurrences at two layers (14–16 km and 16–18 km) inside 30°N–30°S over land and ocean and at 0600 and 1800 are calculated as the percentage of events with clouds identified inside each layer separately. Another independent observation of the thin layer clouds is from CALIPSO [*Winker et al.*, 2003]. CALIPSO was launched on 28 April 2006 into a sunsynchronous 705-km circular polar orbit with 0130 and 1330 local time observations, same as the other A-train satellites. Here the occurrences of thin clouds in the TTL are calculated with two years (July 2006–June 2008) of CALIPSO level-2 layer cloud products [*Vaughan et al.*, 2004]. This product describes tops and bottoms of layer clouds with 5 km horizontal resolution and includes the different types of cirrus clouds [*Nazaryan et al.*, 2008]. To calculate the occurrences of CALIPSO thin clouds, first the clouds are masked at each 100 m interval within the range of the layer cloud top and bottom for each vertical profile. Then total numbers of profiles with cloud at each altitude levels are accumulated on a $1^\circ \times 1^\circ$ grid. Last, the occurrence of CALIPSO thin clouds at each altitude level is derived by dividing the total number of profiles with cloud at the level by the total number of the sampled profiles.

[15] To describe the temperature variation in the TTL, the CPT temperatures and heights are calculated from two years (May 2006–April 2008) of COSMIC data over the tropics [*Anthes et al.*, 2008]. COSMIC includes six constellation satellites using the GPS radio occultation to derive profiles of atmospheric temperature and moisture profile with high vertical resolution and accuracy above the lower troposphere [*Zou et al.*, 1999]. These profiles have 100 m vertical resolution and a full diurnal sampling in the TTL. Because the moisture in the stratosphere has influences on the bending angle and radio refractivity, a one-dimensional variational method (Y. H. Kuo et al., One-dimensional retrieval of temperature and moisture profiles from GPS/MET radio occultation soundings, paper presented at U.S.-Taiwan Bilateral COSMIC Science Workshop, University Corporation for Atmospheric Research, Taipei, Taiwan, 1998) and low-resolution European Centre for Medium-Range Weather Forecasts (ECMWF) analysis are used to estimate the relative contributions of moisture and temperature to correct the "dry" profiles. Here the moisture-corrected profiles are used in order to provide the best estimation of tropopause temperatures and heights. The mean cold point tropopause temperature and heights are shown in Figure 7 with the known coldest CPT over the west Pacific. Lower CPT heights over the Intertropical Convergence Zone (ITCZ) are consistent with previous studies [e.g., *Schmidt et al.*, 2004]. Tropopause temperature is used here as a proxy of temperature in the TTL. However, this may not be a good proxy. It is known that tropopause may be controlled by the radiative balance [*Thuburn and Craig*, 2002]. Here we only focus on understanding the impact of the deep convection on the tropopause temperature over some land regions with intense convection.

3. Results and Discussion

[16] Using all the observations described above, we first discuss further the day versus night differences of CO and water vapor, then describe the diurnal cycles of deep convection, CPT temperatures and heights, and the thin clouds in the TTL.

3.1. Day Versus Night CO Differences

[17] Due to the seasonal variations of the surface CO emission from biomass burning and deep convection,

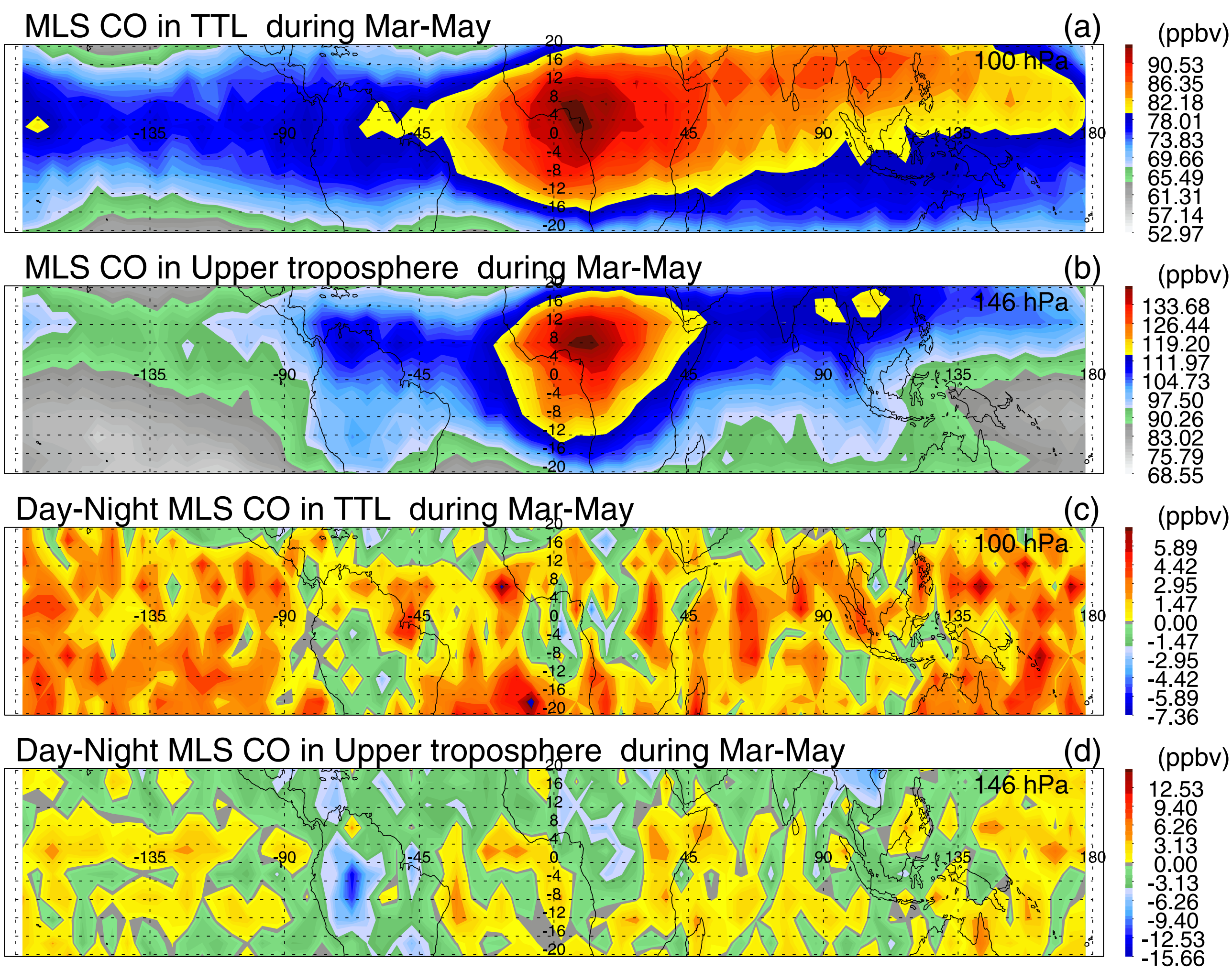

Figure 3. Mean carbon monoxide (CO) mixing ratio and their day versus night differences at 146 and 100 hPa during March–May for 4 years (2005–2008) of AURA MLS observations. (a) Mean carbon monoxide mixing ratio at 100 hPa. (b) Same as Figure 3a, but at 146 hPa. (c) Differences between mean carbon monoxide mixing ratio at 0130 and 1330 at 100 hPa. (d) Same as Figure 3c, but at 146 hPa.

corresponding seasonal variations of day versus night CO differences are expected. Figures 3a and 3b show that during March–May, there is a higher CO concentration in the upper troposphere and the TTL over Africa than over the Amazon because of both active deep convection and the burning season over Africa. In September–November, more deep convection over the Amazon transports more CO into the upper troposphere and the TTL (Figures 4a and 4b). It is clear that during both seasons, there are higher concentrations of CO at 0130 than at 1330 over central Africa and the Amazon in the upper troposphere and the TTL. Note that there is no day versus night regional difference found in the CO at 68 hPa (Figure not shown). It is very rare that deep convection reaches this level [*Liu and Zipser*, 2005].

3.2. Day Versus Night Water Vapor Differences

[18] The day versus night differences of water vapor in the upper troposphere and the TTL during March–May and September–November are shown in Figures 5 and 6. Higher concentration of water vapor in the upper troposphere over central Africa than over Amazon during March–May (Figure 5b) is consistent with the intense deep convection over Africa in this season. Though there is some noise in the day versus night differences, it is clear that in the upper troposphere, there are higher concentrations of water vapor at 0130 than at 1330 in both seasons (Figures 5d and 6d). In the TTL, there are higher concentrations of water vapor at 1330 than at 0130 in both seasons (Figures 5c and 6c).

[19] Note that there is a general higher concentration of water vapor in the northern hemisphere during the day than at night in Figures 1, 5, and 6. There is a general higher concentration of CO in the southern hemisphere during the day than at night in Figures 2, 3 and 4. These inter hemisphere differences are smaller than the accuracy of MLS observations, further investigations are warranted (W. Read, personal communication). However, the general pattern day versus night differences of water vapor and CO over land and ocean are clearly shown in two separate seasons.

3.3. Geodiurnal Variation of Deep Convection and Tropopause Temperature and Height

[20] To describe the regional variations of the diurnal cycles of deep convection over tropics, the occurrence of TRMM PR 20 dBZ reaching 14 km and the VIRS T_{B11} < 210 K are

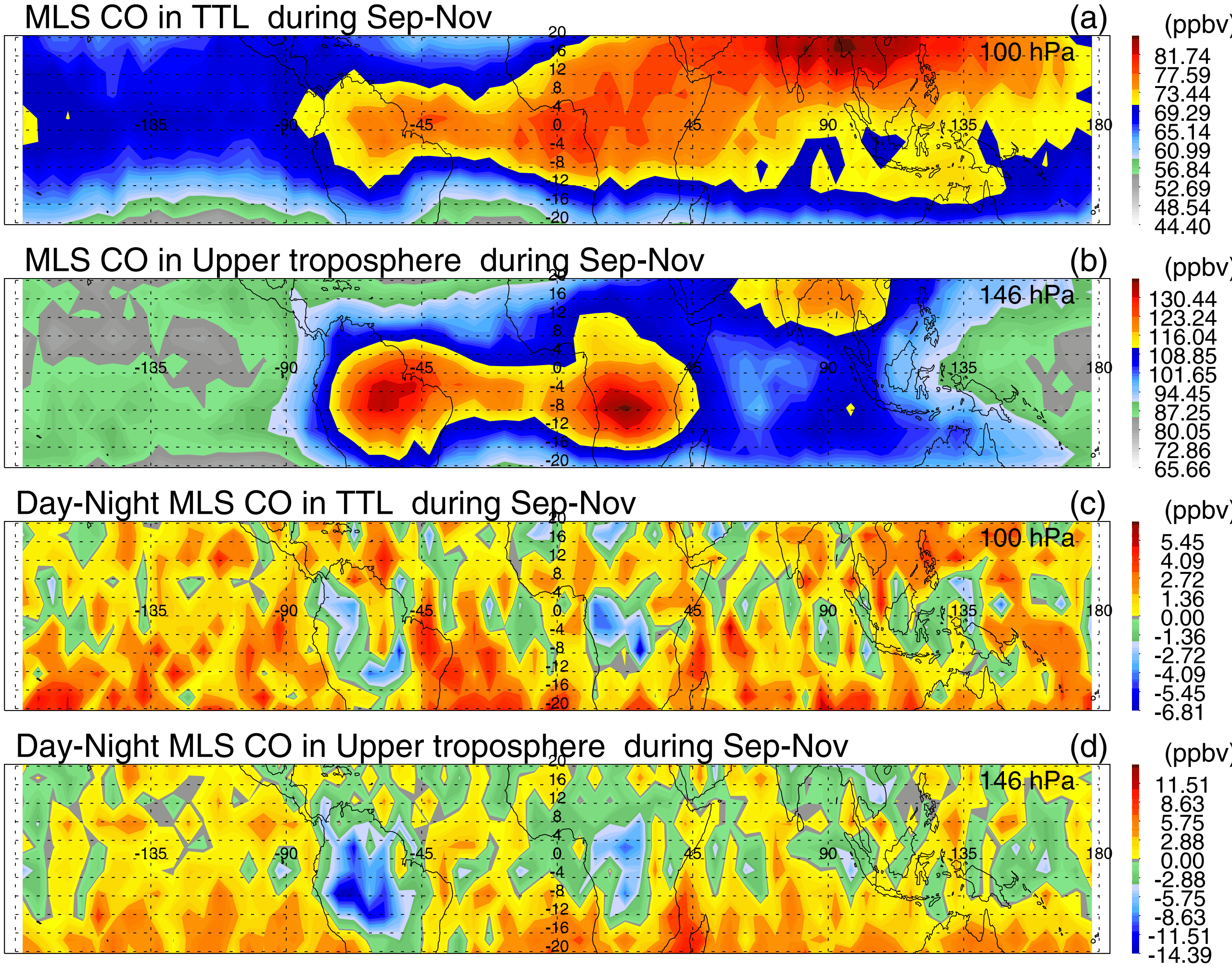

Figure 4. Mean carbon monoxide (CO) mixing ratio and their day versus night differences at 146 and 100 hPa during September–November for 4 years (2005–2008) of AURA MLS observations. (a) Mean carbon monoxide mixing ratio at 100 hPa. (b) Same as Figure 4a, but at 146 hPa. (c) Differences between mean carbon monoxide mixing ratio at 0130 and 1330 at 100 hPa. (d) Same as Figure 4c, but at 146 hPa.

calculated for 10° longitudinal boxes within 10°S–10°N for each two-hour local time bin. Then the Hovmoller type geodiurnal variation of tropical deep convection are shown with the longitude versus local time distribution of occurrences of VIRS T_{B11} < 210 K and PR 20 dBZ at 14 km (Figures 8a and 8b). There are four regions with frequent deep convective clouds, including central Africa, Amazon, maritime continent and the west Pacific. Consistent with the known diurnal cycles of deep convection, there are more deep convective clouds in the afternoon over land and more in the early morning over ocean. The only difference between Figures 8a and 8b is the lower frequency of PR 20 dBZ at 14 km over the west Pacific compared with the high frequency of cold clouds over the same region. The high sea surface temperature and the abundant moisture over the west Pacific is thermodynamically consistent with a high level of neutral buoyancy. As a result, convection over the region can easily reach high altitudes and produce extensive areas cold clouds. However, convection over this region is relatively weak and only rarely lifts large precipitation particles to high altitudes with radar echoes detectable by the PR [*Liu et al.*, 2007b].

[21] In regions such as subtropical South America, intense deep convection may have a strong impact on the tropopause temperature [e.g., *Pommereau and Held*, 2007]. For comparison, the mean CPT heights and temperature are calculated on the same grids and local time bins as Figure 8a. The geodiurnal hovmoller diagrams of CPT temperature and height are shown in Figures 8c and 8d. There are similarities between the patterns of geodiurnal variations of deep convection (Figure 8a) and that of the mean CPT temperature (Figure 8c). First, consistent with Figure 7a, CPT temperatures are lower over the four regions with frequent cold clouds. Over central Africa, the coldest CPT temperature in the afternoon (Figure 8c) seems to correspond with the frequent convective clouds (Figures 8a and 8b). However, the coldest CPT temperature in early morning over Amazon is not consistent with the more frequent convection in the afternoon. In contrast with the CPT temperature, the geodiurnal variation of the mean CPT heights in Figure 8d does not show a general correlation with deep convection inferred in Figures 8a and 8b, except positive correlations over some land regions such as central Africa. CPT height may also be controlled by other factors,

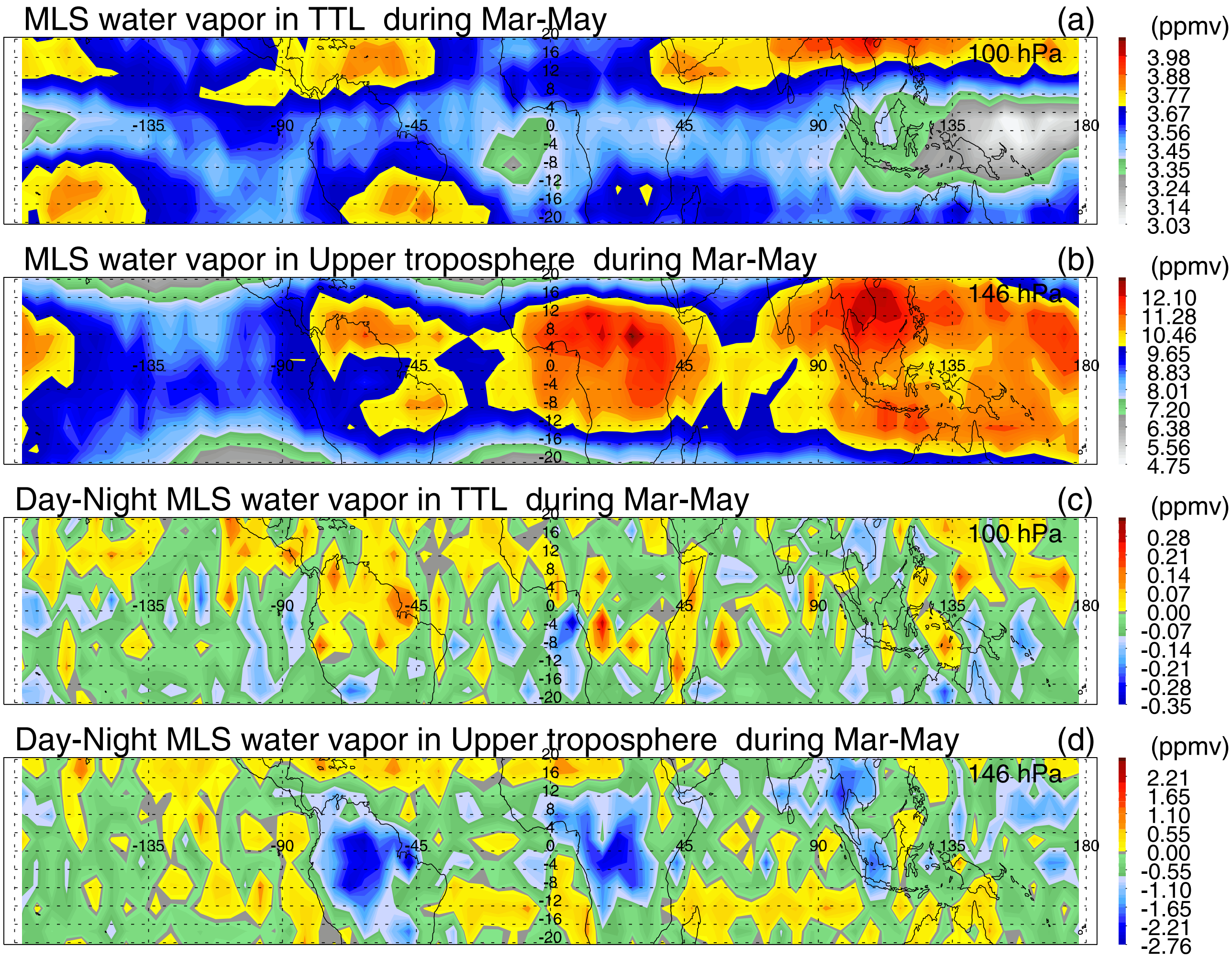

Figure 5. Mean water vapor mixing ratio and their day versus night differences at 146 and 100 hPa during March–May for 4 years (2005–2008) of AURA MLS observations. (a) Mean water vapor mixing ratio at 100 hPa. (b) Same as Figure 5a, but at 146 hPa. (c) Differences between mean water vapor mixing ratio at 0130 and 1330 at 100 hPa. (d) Same as Figure 5c, but at 146 hPa.

such as the day and night radiative balance [*Thuburn and Craig*, 2002].

3.4. Day Versus Night Thin Cloud Occurrence

[22] The geographical distribution of the mean fractional occurrence of CALIPSO layer clouds at 16 km at 0130 and 1330 is shown in Figures 9a and 9b. In general, there are more layer clouds detected by CALIPSO at 1330 (Figure 9b) than at 0130 (Figure 9a). It is known that CALIPSO observes more layer clouds at 0130 than at 1330 due to higher sensitivity and better signal-to-noise ratio at night [*Nazaryan et al.*, 2008]. So it is not fair to directly compare the absolute values of fractional occurrences of CALIPSO layer clouds at 1330 and 0130. However, it is fair to compare the occurrences of clouds over two different regions at the same time. At 1330 there are much more layer clouds over tropical ocean than over land at 16 km (Figure 9a). However, at 0130 the fractional occurrences of layer clouds over land are close to that over ocean. It is known that the diurnal cycles of deep convection and clouds are weak over ocean [*Liu and Zipser*, 2008]. If we use the fractional occurrence of layer clouds over ocean as a rough constant reference for clouds over land at 0130 and at 1330, the layer clouds at 16 km over central Africa and Amazon could occur up to 30–40% more frequently at 0130 than at 1330. This is more obvious in Figures 9c and 9d: At 1330 the mean occurrence of CALIPSO layer clouds in the TTL over 30°S–30°N land is close to that over 30°S–30°N ocean (Figure 9c). However, at 0130, the mean occurrence of CALIPSO layer clouds over land is 5% larger than that over ocean, which also means that there are 20–30% more clouds over land than over ocean.

[23] For comparison, the occurrences of SAGE II thin clouds at 14–16 km and 16–18 km layers over 30°S–30°N land and ocean are calculated for 1800 and 0600 local time separately (cross symbols in Figures 9c and 9d). In general, SAGE II detects more thin clouds at 1800 than at 0600, especially over land. At 0600, the mean occurrence of SAGE II thin clouds in the TTL over 30°S–30°N land is close to that over 30°S–30°N ocean (Figure 9d). However, at 1800, the mean occurrence of SAGE II thin clouds over land is larger than that over ocean. Considering the weak diurnal cycle over ocean, if we use occurrence of layer clouds over ocean as a rough constant reference, Figures 9c and 9d suggests that there are more thin clouds in the

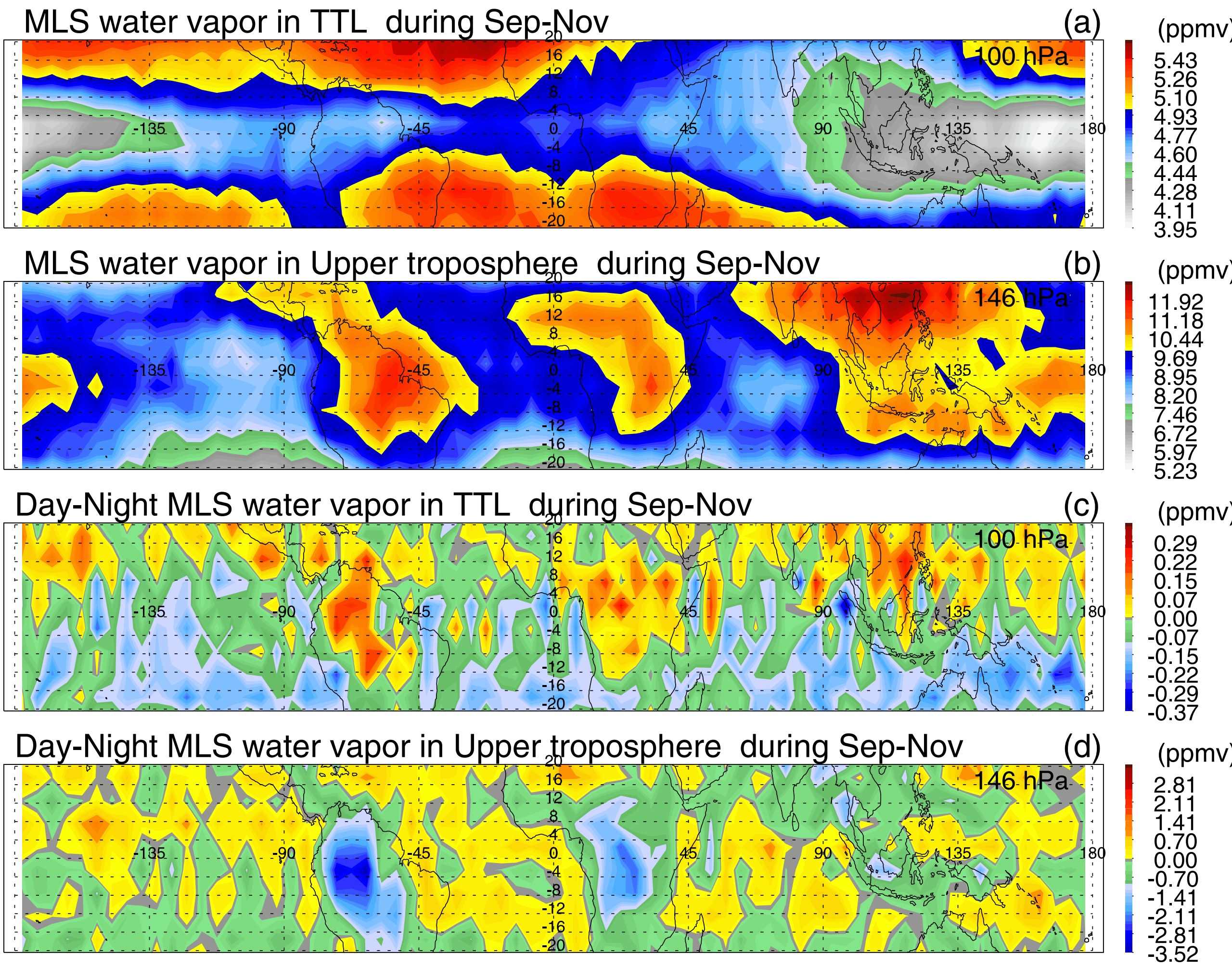

Figure 6. Mean water vapor mixing ratio and its day versus night differences at 146 and 100 hPa during September–November for 4 years (2005–2008) of AURA MLS observations. (a) Mean water vapor mixing ratio at 100 hPa. (b) Same as Figure 6a, but at 146 hPa. (c) Differences between mean water vapor mixing ratio at 0130 and 1330 at 100 hPa. (d) Same as Figure 6c, but at 146 hPa.

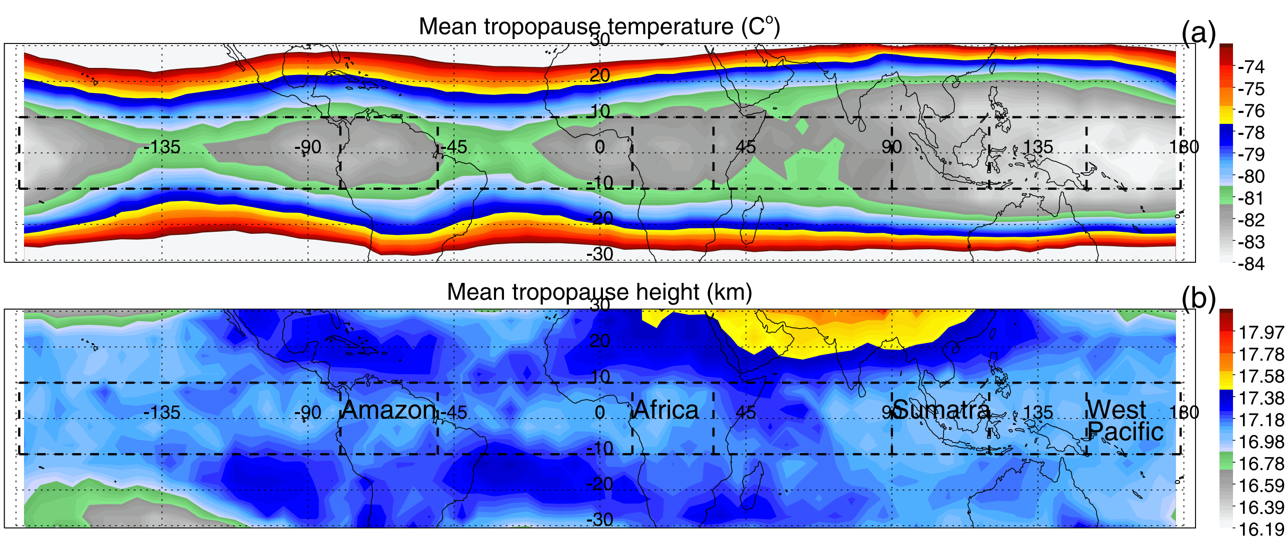

Figure 7. Mean cold point tropopause (a) temperature and (b) height from 2 years (May 2006–April 2008) of COSMIC GPS soundings.

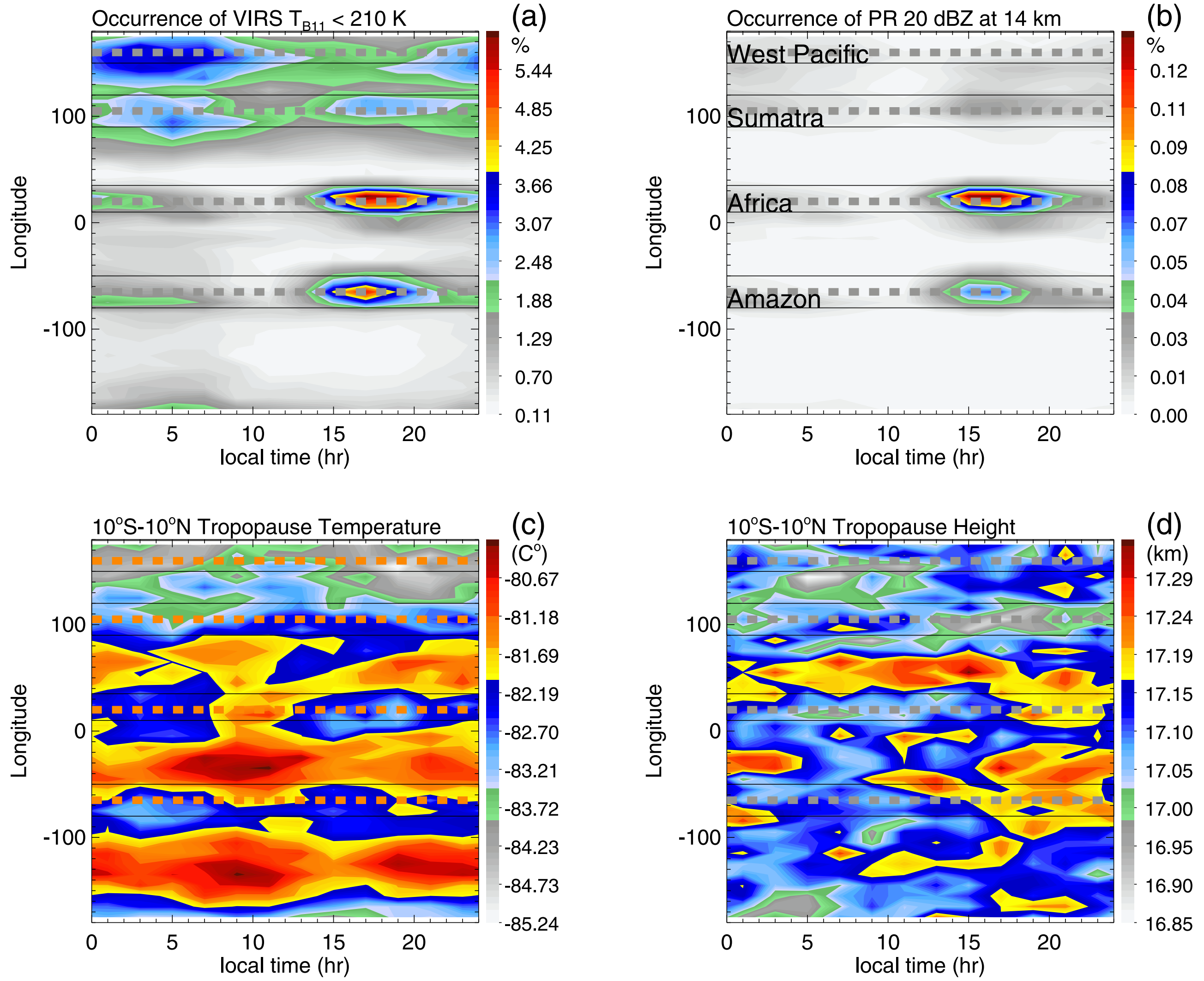

Figure 8. Geodiurnal variations of deep convection and tropopause temperature and height for10°S–10°N. (a) Geodiurnal variation of occurrence of VIRS $T_{B11} < 210$ K. (b) Geodiurnal variation of occurrence of PR 20 dBZ reaching at 14 km. (c) Geodiurnal variation of mean cold point tropopause temperature identified from COSMIC GPS temperature profiles. (d) Same as Figure 8c, but for mean cold point tropopause height. Figures 8a and 8b are generated using 10 years (1998–2007) of TRMM observations. Figures 8c and 8d are generated using 2 years (May 2006–April 2008) of COSMIC observations. All panels are generated with 10° longitude and 2-hour bins. Four bands of regions are Central Africa, Amazon, West Pacific, and Sumatra, as shown in Figure 7b.

afternoon and at night than during early morning and noon over tropical land.

3.5. Discussion

[24] After all the diurnal variations of deep convection, thin clouds, and CPT temperature and heights are presented, how do we relate these results to the day versus night differences of the water vapor and CO concentrations in the TTL as shown in Figures 1 and 2? The first step is to discuss 146 hPa and100 hPa separately.

3.5.1. In the Upper Troposphere Below the TTL

[25] Over tropical land, deep convective systems generally start to develop in the early afternoon and continuously transport air with high water vapor and CO concentrations vertically from the lower troposphere to the near bottom of the TTL well into the night. Some large size Mesoscale Convective Systems (MCS) may keep developing through the night even until the early morning [*Nesbitt and Zipser*, 2003]. As shown in Figures 10a and 10b, at 1330 cold clouds from deep convection just start to develop over central Africa and Amazon. For many hours, well into the night, deep convective systems may continuously transport both water vapor and CO to the 146 hPa level. Therefore at 0130, there are higher concentrations of water vapor and CO at 146 hPa over these regions (Figures 1d and 2d). Because of horizontal mixing and less vertical transport with less frequent deep convection in the morning, the concentrations of water vapor and CO decrease and may reach their minima near noon, before the next diurnal cycle of afternoon convection begins replenishing the water vapor and CO to the upper

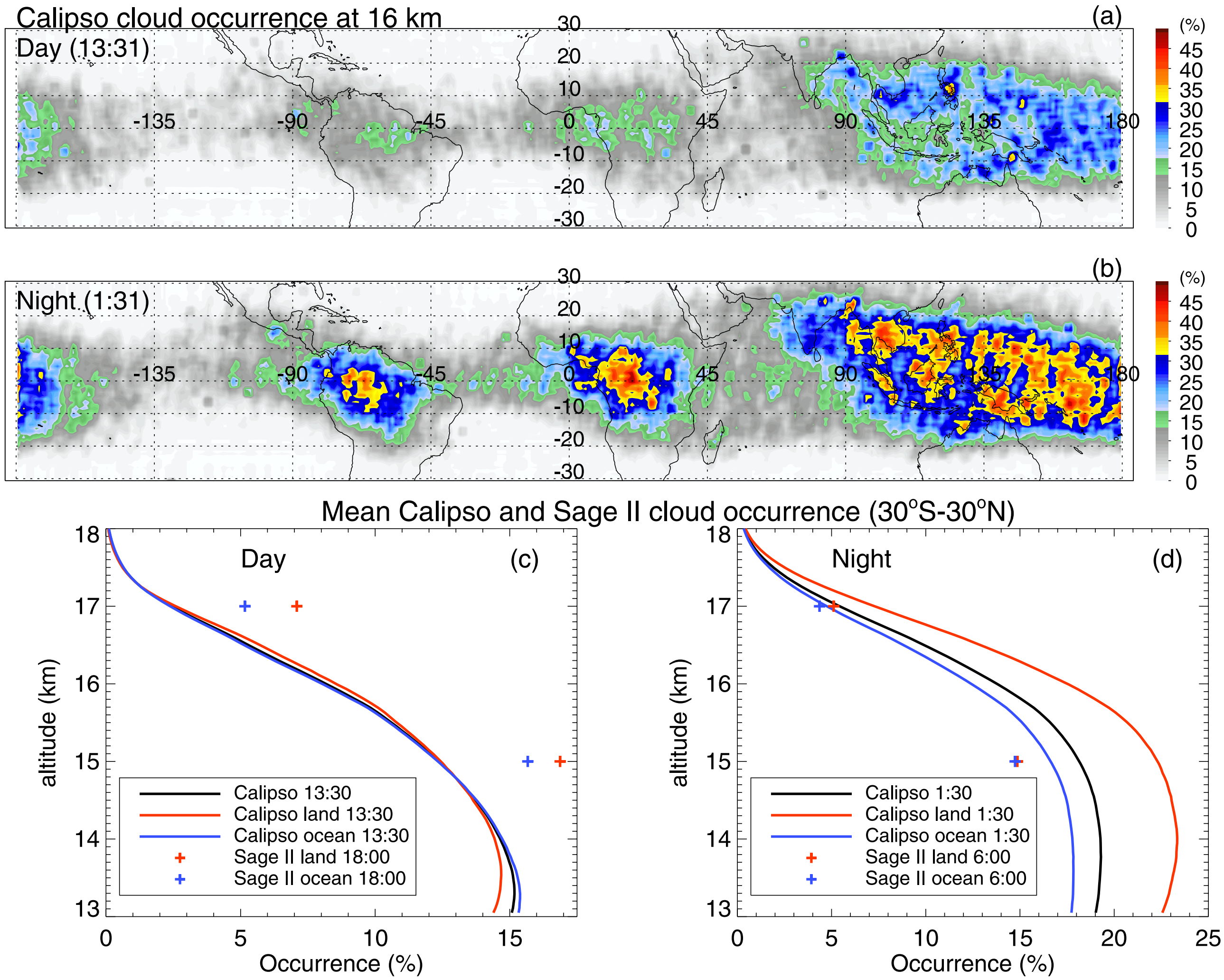

Figure 9. Mean cloud occurrences in the TTL from 2 years (July 2006–June 2008) of Calipso and 16 years (1984–1991, 1996–2005) of SAGE II observations. (a) Fractional occurrence of Calipso layer clouds at 16 km and 1330 local time. (b) Same as Figure 9a, but at 0330 local. (c) Vertical profiles of mean occurrence of Calipso layer clouds (lines) over tropical land and ocean (30°S–30°N) at 1330 local time and the mean occurrence of SAGE II thin clouds over tropical land and ocean (30°S–30°N) at 1800 local time (cross symbols). (d) Same as Figure 9c, but for Calipso clouds at 0130 local time and SAGE II clouds at 0600 local time.

troposphere again. This is consistent with higher concentrations of water vapor and CO at 0130 than at 1330 at 146 hPa over land in Figures 1d and 2d.

[26] Over tropical oceans, deep convection has a weak diurnal cycle, opposite phase tothat over land [e.g., *Augustine*, 1984; *Hall and Vonder Haar*, 1999; *Nesbitt and Zipser*, 2003; *Liu and Zipser*, 2008]. More frequent deep convective systems transport more water vapor to the upper troposphere during the morning. Therefore there are a somewhat higher concentrations of water vapor at 1330 than at 0130 at 146 hPa over tropical ITCZ ocean.

3.5.2. In the TTL

[27] There are only a few strong deep convective systems that can reach into the TTL and some of them can even penetrate the CPT over tropical land [*Liu and Zipser*, 2005; *Corti et al.*, 2008]. These convective systems have a diurnal cycle with a greater amplitude than the diurnal cycle of general convection over land. These convective systems may directly inject CO into the TTL during afternoon until the mid night and lead to a higher concentration of CO at 0130 than at 1330 over tropical land as shown in Figure 2c. However, what about the water vapor transported into the TTL along with CO? It is clear that there are lower concentrations of water vapor at 0130 than at 1330 at 100 hPa over tropical land in Figure 1c which is in the opposite to the CO in Figure 2c. The most plausible explanation is that most of the water vapor transported into the TTL along with CO has been converted into ice phase.

[28] There are two possible ways for transported water vapor to be converted into the solid phase in the TTL. The first is that the water vapor in the core of deep convection undergoes deposition onto ice particles because the adiabatic cooling in the core of deep convection above the level of neutral buoyancy leads to a lower temperature in the core than the ambient air in the TTL [*Danielsen*, 1982; *Sherwood and Dessler*, 2003; *Salby et al.*, 2003]. The counterargument

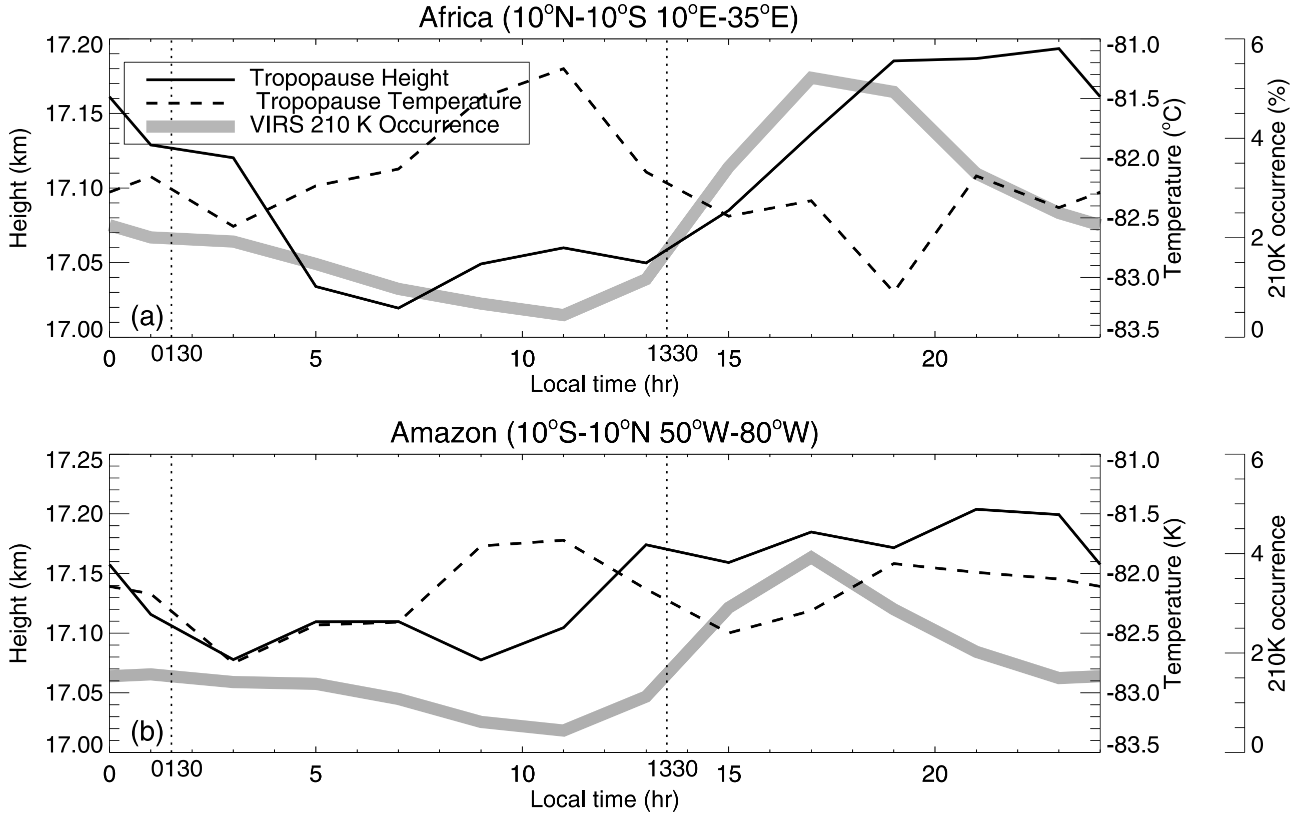

Figure 10. Diurnal cycles of occurrence of TRMM VIRS T_{B11} < 210 K, mean cold point tropopause temperature, and height from COSMIC GPS temperature profiles over (a) central Africa (10°N–10°S, 10°E–30°E) and (b) Amazon (10°N–10°S, 50°W–80°W).

on this is that the occurrence of deep convection reaching the TTL is too low, and also that the detrainment of the ice particles from the top of the deep convection may rehydrate the TTL. The second explanation is the "freeze and dry" in the TTL during the lifting and cooling from the deep convection and its induced gravity waves [*Potter and Holton*, 1995]. Because the TTL is often saturated with respect to ice [*Jensen et al.*, 2005] the pileus clouds may form easily by the lifting and cooling [*Garrett et al.*, 2006]. The lifting and cooling is evident in the diurnal cycles of CPT temperature and height over Africa in Figure 10a: the mean CPT temperature decreases and the mean CPT height increases when occurrence of deep convection increases in the afternoon over central Africa. The amount of lifting and cooling may be directly related to the strength of the deep convection: the amplitude of the diurnal variation of CPT temperature and height over Amazon is much lower than those over Africa because Amazonian deep convection is less intense.

[29] Both hypotheses are consistent with the observed day versus night differences of water vapor at 100 hPa over land shown in Figure 1c. Using the hypothesis of adiabatic cooling and drying in the cores of deep convection, the continuous cooling in the core of the deep convection over Africa and Amazon during the afternoon till mid night may lead to dryer air in the TTL at 0130 than at 1330. This is consistent with the lower water vapor concentration at 0130 in Figure 1c. Using the hypothesis of the lifting and cooling by gravity waves, deep convection lifts and cools and soon saturates the TTL in the afternoon over land. Then it is the temperature that controls the concentration of the water vapor in the TTL. However, the mean CPT over both Africa and the Amazon at 1330 are only a little warmer than those at 0130. Then what leads to the higher concentrations of water vapor at 1330 as shown in Figure 1c? Since we are using CPT as a proxy of the TTL temperature, detailed observations of the diurnal variation of temperature in the TTL are required to answer this question.

[30] Both hypotheses lead to the cooling of the TTL. As the by-product of cooling and freezing, more and more thin clouds are generated during the afternoon and evening and may reach maximum extent near midnight over land. When deep land convection dissipates in the early morning, the lifted TTL starts to descend and warms up. Some thin clouds dissipate when the ice particles start to sublimate to maintain saturation under a warmer temperature. As a result, there are less thin clouds through most of the day. This is consistent with the diurnal variation of occurrence of thin cloud in the TTL over land in Figure 9.

[31] There is one key in the process of converting the water vapor into the ice clouds during the cooling: saturation of the TTL. To demonstrate this, the mean occurrences of relative humidity respect to ice (RHI) greater than 100% are calculated from 4 years of MLS data. As shown in Figure 11, there is higher occurrence of RHI > 100% in the TTL than in the upper troposphere. There are higher occurrences of RHI > 100% in the upper troposphere and the TTL over Africa and Amazon at 0130 than at 1330. This is consistent with more thin clouds at 0130 in the TTL over land in

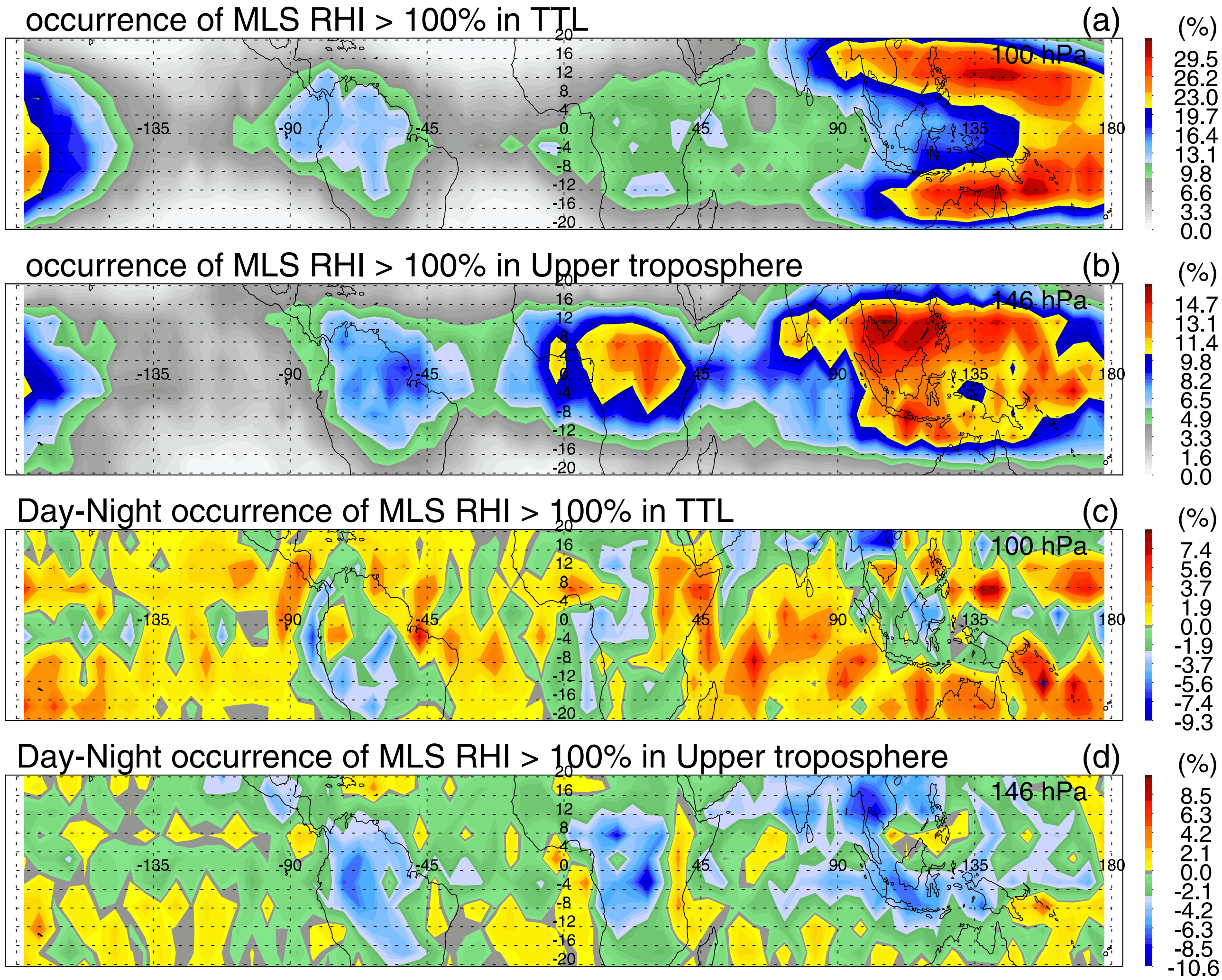

Figure 11. Fractional occurrence of water vapor relative humidity with respect to ice (RHI) greater than 100% and their day versus night differences at 146 and 100 hPa for 4 years (2005–2008) of AURA MLS observations. (a) Fractional occurrence of RHI > 100% at 100 hPa. (b) Same as Figure 11a, but at 146 hPa. (c) Differences between fractional occurrence of RHI > 100% at 0130 and 1330 at 100 hPa. (d) Same as Figure 11c, but at 146 hPa.

Figure 9. However, since the quality of the RHI retrievals depends on the water vapor retrievals and the temperature profiles with low vertical resolution, these results need to be considered as tentative.

[32] An alternative source of water vapor in the TTL is worth mentioning. Convective overshooting may transport ice particles into the TTL, which would later sublimate and hydrate the TTL as shown by *Corti et al.* [2008] and *Khaykin et al.* [2008]. This process could help saturate the TTL when the TTL is initially unsaturated. However, after the TTL reaches saturation, this process would no longer introduce water vapor into the TTL.

[33] Even with all the above observations, the mechanism of water vapor transport and freezing is still not clear. However, all the observations suggest that the diurnal variations of thin cloud, water vapor, deep convection and the temperature in the TTL are correlated, important in understanding the process and worth further investigation. More detailed observations covering the diurnal cycles of thin cloud, water vapor and temperature in the TTL are required in the future.

4. Summary

[34] 1. Large day versus night differences of water vapor and CO concentrations in the upper troposphere over tropical land are consistent with the strong diurnal cycle of vertical transport by deep convection.

[35] 2. The day versus night differences of CO concentration in the TTL shown by MLS observations may be interpreted as the result of the vertical transport by a few deep convective systems reaching into the TTL. However, the day versus night differences of water vapor concentration is more likely interpreted as a result of the diurnal cycle of temperature in a saturated TTL.

[36] 3. The positive correlation between the diurnal cycle of the occurrence of deep convective clouds and that of the tropopause height, and the negative correlation between the

diurnal cycle of deep convection and that of the tropopause temperature over central Africa are consistent with the lifting and cooling of the TTL by deep convection. The amount of lifting may be related to the strength of the deep convection.

[37] 4. There are up to 30% more thin clouds at 0130 than at 1330, more in the afternoon than in the morning over tropical land. This is consistent with the "freeze and dry" process driven by the diurnal variation of the temperature in the TTL, which is largely influenced by the diurnal cycle of deep convection over the tropical land.

[38] 5. The signatures of the diurnal cycle of deep convection are embedded in the day versus night differences of water vapor, CO, thin clouds, tropopause temperature and height over tropical land. However, the twice daily sampling of the water vapor, CO and thin cloud by A-train satellites is a handicap to full understanding of the relations among them. Observations with full diurnal sampling are needed for understanding the shorter timescale physical processes in the troposphere-stratosphere exchange.

[39] **Acknowledgments.** We thank three anonymous reviewers for valuable suggestions to improve this paper, William Read for the insight to the MLS observations, and especially John Kwiatkowski and the rest of the TRMM Science Data and Information System (TDSIS, at NASA Goddard Space Flight Center, Greenbelt, MD) for data processing assistance. This research was supported by NASA's Precipitation Measurement Mission grants NAG5-13628 and NN-H-06-Z-DA-001-N under the direction of Ramesh Kakar and NNX08AK28G under Erich Stocker.

References

Anthes, R. A., et al. (2008), The COSMIC/FORMOSAT-3 mission: Early results, *Bull. Am. Meteorol. Soc.*, *89*, 313–333.

Augustine, J. A. (1984), The diurnal variation of large-scale inferred rainfall over the tropical Pacific Ocean during August 1979, *Mon. Weather Rev.*, *112*, 1745–1751.

Brewer, A. M. (1949), Evidence for a world circulation provided by the measurements of helium and water vapor distribution in the stratosphere, *Q. J. R. Meteorol. Soc*, *75*, 351–363.

Corti, T., et al. (2008), Unprecedented evidence for deep convection hydrating the tropical stratosphere, *Geophys. Res. Lett.*, *35*, L10810, doi:10.1029/2008GL033641.

Dai, A. (2001), Global precipitation and thunderstorm frequencies: Part II. Diurnal variations, *J. Clim.*, *14*, 1112–1128.

Danielsen, E. F. (1982), A dehydration mechanism for the stratosphere, *Geophys. Res. Lett.*, *9*, 605–608.

Dessler, A. E., S. P. Palm, W. D. Hart, and J. D. Spinhirne (2006), Tropopause-level thin cirrus coverage revealed by ICESat/GLAS, *J. Geophys. Res.*, *111*, D08203, doi:10.1029/2005JD006586.

Dessler, A. E., T. F. Hanisco, and S. Fueglistaler (2007), Effects of convective ice lofting on H_2O and HDO in the tropical tropoause layer, *J. Geophys. Res.*, *112*, D18309, doi:10.1029/2007JD008609.

Duncan, B. N., R. V. Martin, A. C. Staudt, R. Tevich, and J. A. Logan (2003), Interannual and seasonal variability of biomass burning emissions constrained by satallite observations, *J. Geophys. Res.*, *108*(D2), 4100, doi:10.1029/2002JD002378.

Fueglistaler, S., and P. H. Haynes (2005), Control of interannual and longer term variability of stratospheric water vapor, *J. Geophys. Res.*, *110*, D24108, doi:10.1029/2005JD006019.

Garrett, T., J. Dean-Day, C. Liu, B. K. Barnett, G. G. Mace, D. G. Baumgardner, C. R. Webster, T. Paul Bui, W. R. Read, and P. Minnis (2006), Convective formation of pileus cloud near the tropopause, *Atmos. Chem. Phys.*, *6*, 1185–1200.

Gettelman, A., and T. Birner (2007), Insights into tropical tropopause layer precesses using global models, *J. Geophys. Res.*, *112*, D23104, doi:10.1029/2007JD008945.

Gettelman, A., M. L. Salby, and F. Sassi (2002), Distribution and influence of convection in the tropical tropopause region, *J. Geophys. Res.*, *107*(D10), 4080, doi:10.1029/2001JD001048.

Hall, T. J., and T. H. Vonder Haar (1999), The diurnal cycle of west Pacific deep convection and its relation to the spatial and temporal variation of tropical MCSs, *J. Atmos. Sci.*, *56*, 3401–3415.

Hartmann, D. L., J. R. Holton, and Q. Fu (2001), The heat balance of the tropical tropopause, cirrus, and stratospheric dehydration, *Geophys. Res. Lett.*, *28*, 1969–1972.

Jensen, E. J., and L. Pfister (2004), Transport and freeze-drying in the tropical tropopause layer, *J. Geophys. Res.*, *109*, D02207, doi:10.1029/2003JD004022.

Jensen, E. J., et al. (2005), Ice supersaturations exceeding 100% at the cold tropical tropopause: Implications for cirrus formation and dehydration, *Atmos. Chem. Phys.*, *5*, 851–862.

Jensen, E. J., A. S. Ackerman, and J. A. Smith (2007), Can overshooting convection dehydrate the tropical tropopause layer?, *J. Geophys. Res.*, *112*, D11209, doi:10.1029/2006JD007943.

Jiang, J. H., N. J. Livesey, H. Su, L. Neary, J. C. McConnell, and N. A. Richards (2007), Connecting surface emissions, convective uplifting, and long-range transport of carbon monoxide in the upper-troposphere: New observations from the Aura Microwave Limb Sounder, *Geophys. Res. Lett.*, *34*, L18812, doi:10.1029/2007GL030638.

Kar, J., et al. (2004), Evidence of vertical transport of carbon monoxide from Measurements of Pollution in the Troposphere (MOPITT), *Geophys. Res. Lett.*, *31*, L23105, doi:10.1029/2004GL021128.

Kent, G. S., D. M. Winker, M. T. Osborn, and K. M. Skeens (1993), A model for the separation of cloud and aerosol in SAGE II occultation data, *J. Geophys. Res.*, *98*, 20,725–20,735.

Khaykin, S., J.-P. Pommereau, L. Korshunow, V. Yushkov, J. Nielsen, N. Larsen, T. Christensen, A. Garnier, A. Lukyanov, and E. Williams (2008), Hydration of the lower stratophsere by ice crystal geysers over land convective systems, *Atmos. Chem. Phys.*, *8*, 15,463–15,490.

Kistler, R., et al. (2001), The NCEP-NCAR 5-year reanalysis: Monthly means CD-ROM and documentation, *Bull. Am. Meteorol. Soc.*, *82*, 247–267.

Kummerow, C., W. Barnes, T. Kozu, J. Shiue, and J. Simpson (1998), The Tropical Rainfall Measuring Mission (TRMM) Sensor Package, *J. Atmos. Ocean. Techol.*, *15*, 809–817.

Liu, C., and E. Zipser (2005), Global distribution of convection penetrating the tropical tropopause, *J. Geophys. Res.*, *110*, D23104, doi:10.1029/2005JD006063.

Liu, C., and E. Zipser (2008), Diurnal cycles of precipitation, clouds and lightning in the tropics from 9 years of TRMM observations, *Geophys. Res. Lett.*, *35*, L04819, doi:10.1029/2007GL032437.

Liu, C., E. Zipser, T. Garrett, J. H. Jiang, and H. Su (2007a), How do the water vapor and carbon monoxide "tape recorders" start near the tropical tropopause?, *Geophys. Res. Lett.*, *34*, L09804, doi:10.1029/2006GL029234.

Liu, C., E. Zipser, and S. W. Nesbitt (2007b), Global distribution of tropical deep convection: Different perspectives using infrared and radar as the primary data source, *J. Clim.*, *20*, 489–503.

Liu, C., E. Zipser, D. Cecil, S. W. Nesbitt, and S. Sherwood (2008), A cloud and precipitation feature database from 9 years of TRMM observations, *J. Appl. Meteorol. Clim.*, *47*, 2712–2728.

Livesey, N. J., W. V. Snyder, W. G. Read, and P. A. Wagner (2006), Retrieval algorithms for the EOS Microwave Limb Sounder (MLS) instrument, *IEEE Trans. Geosci. Remote Sens.*, *44*, 1144–1155.

Livesey, N. J., et al. (2007), Earth Observing Systems (EOS) Microwave Limb Sounder (MLS) Version 2.2 level 2 data quality and description document, version 2.2 $\times$ $-$1.0a, Jet Propulsion Laboratory.

Massie, S., A. Gettelman, W. Randel, and D. Baumgardner (2002), Distribution of tropical cirrus in relation to convection, *J. Geophys. Res.*, *107*(D21), 4591, doi:10.1029/2001JD001293.

McCormick, M. P., L. W. Thomason, and C. R. Trepte (1995), Atmospheric effects of the Mount Pinatubo eruption, *Nature*, *373*, 399–404.

McFarquhar, G. M., A. J. Heymsfield, J. Spinhirne, and B. Hart (2000), Thin and subvisual tropopause tropical cirrus: Observations and radiative impacts, *J. Atmos. Sci.*, *57*, 1841–1853.

Nazaryan, H., M. P. McCormick, and W. P. Menzel (2008), Global characterization of cirrus clouds using CALIPSO data, *J. Geophys. Res.*, *113*, D16211, doi:10.1029/2007JD009481.

Negri, A. J., T. L. Bell, and L. Xu (2002), Sampling of the diurnal cycle of precipitation using TRMM, *J. Atmos. Ocean. Technol.*, *19*, 1333–1344.

Nesbitt, S. W., and E. J. Zipser (2003), The diurnal cycle of rainfall and convective intensity according to three years of TRMM measurements, *J. Clim.*, *16*, 1456–1475.

Newell, R. E., and S. Gould-Stewart (1981), A stratosperic fountain?, *J. Atmos. Sci.*, *38*, 2789–2796.

Pommereau, J.-P., and G. Held (2007), Is there a stratospheric fountain?, *Atmos. Chem. Phys. Discuss.*, *7*, 8933–8950.

Potter, B. E., and J. R. Holton (1995), The role of monsoon convection in the dehydration of the lower tropical stratosphere, *J. Atmos. Sci.*, *52*, 1034–1050.

Randel, W. J., F. Wu, and D. J. Gaffen (2000), Interannual variability of the tropical tropopause derived from radiosonde data and NCEP reanalysis, *J. Geophys. Res.*, *105*, 15,509–15,523.

Randel, W. J., F. Wu, H. Vomel, G. W. Nedoluha, and P. Forster (2006), Decreases in stratospheric water vapor after 2001: Links to changed in

the tropical tropopause and the Brewer-Dobson circulation, *J. Geophys. Res.*, *111*, D12312, doi:10.1029/2005JD006744.
Read, W. G., M. J. Schwartz, A. Lambert, H. Su, N. J. Livesey, W. H. Daffer, and C. D. Boone (2008), The roles of convection, extratropical mixing, and in situ freeze-drying in the tropical tropopause layer, *Atmos. Chem. Phys.*, *8*, 6051–6067.
Ricaud, P., B. Barret, J.-L. Attie, E. Motte, E. Le Flochmoen, H. Teyssedre, V.-H. Peuch, N. Livesey, A. Lambert, and J.-P. Pommereau (2007), Impact of land convection on troposphere-stratosphere exchange in the tropics, *Atmos. Chem. Phys.*, *7*, 5639–5657.
Salby, M., F. Sassi, P. Callaghan, W. Read, and H. Pumphrey (2003), Fluctuations of cloud, humidity, and thermal structure near the tropical tropopause, *J. Clim.*, *16*, 3428–3446.
Sassen, K., M. K. Griffin, and G. C. Dodd (1989), Optical scattering and microphysical properties of subvisible cirrus clouds, and climatic implication, *J. Atmos. Sci.*, *28*, 91.
Schmidt, T., J. Wichert, G. Beyerle, and C. Reigber (2004), Tropical tropopause parameters derived from GPS radio occultation measurements with CHAMP, *J. Geophys. Res.*, *109*, D13105, doi:10.1029/2004JD004566.
Schoeberl, M. R., B. N. Duncan, A. R. Douglass, J. Waters, N. Livesey, W. Read, and M. Filipiak (2006), The carbon monoxide tape recorder, *Geophys. Res. Lett.*, *33*, L12811, doi:10.1029/2006GL026178.
Sherwood, S. C., and A. E. Dessler (2003), Convective mixing near the tropical tropopause: Insights from seasonal variations, *J. Atmos. Sci.*, *60*, 2674–2685.
Thuburn, J., and G. Craig (2002), On the temperature structure of the tropical substratosphere, *J. Geophys. Res.*, *107*(D2), 4017, doi:10.1029/2001JD000448.
Vaughan, M., et al. (2004), Fully automated analysis of space-based lidar data: An overview of the CALIPSO retrieval algorithms and data products, *Proc. SPIE*, *5575*, doi:10.1117/12.572004.
Wang, P. H., P. Minnis, M. P. McCormick, G. S. Kent, and K. M. Skeens (1996), A 6-year climatology of cloud occurrence frequency from stratospheric aerosol and gas experiment II observations (1985–1990), *J. Geophys. Res.*, *101*, 29,407–29,429.
Winker, D. M., J. R. Pelon, and M. P. McCormick (2003), The CALIPSO mission: Spaceborne lidar for observation of aerosols and clouds, *Proc. SPIE*, *4893*, 1–11.
Wu, D. L., W. G. Read, A. E. Dessler, S. C. Sherwood, and J. H. Jiang (2005), UARS MLS cloud ice measurements and implications for H_2O transport near the tropopause, *J. Atmos. Sci.*, *62*, 518–530.
Yang, G.-Y., and J. Slingo (2001), The diurnal cycle in the tropics, *Mon. Weather Rev.*, *129*, 784–801.
Zou, X., et al. (1999), A ray-tracing operator and its adjoint for the use of GPS/MET refraction angle measurements, *J. Geophys. Res.*, *104*, 22,301–22,318.

C. Liu and E. J. Zipser, Department of Meteorology, University of Utah, 135 S 1460 E, Room 819, Salt Lake City, UT 84112-0110, USA. (liu.c.t@utah.edu)